



## Raman Spectrum of Graphite

F. Tuinstra and J. L. Koenig

Citation: *The Journal of Chemical Physics* **53**, 1126 (1970); doi: 10.1063/1.1674108

View online: <http://dx.doi.org/10.1063/1.1674108>

View Table of Contents: <http://scitation.aip.org/content/aip/journal/jcp/53/3?ver=pdfcov>

Published by the AIP Publishing

### Articles you may be interested in

[Raman Spectrum of Graphite Layers in Indian Coal](#)

AIP Conf. Proc. **1391**, 140 (2011); 10.1063/1.3646804

[Origin of the D line in the Raman spectrum of graphite: A study based on Raman frequencies and intensities of polycyclic aromatic hydrocarbon molecules](#)

J. Chem. Phys. **114**, 963 (2001); 10.1063/1.1329670

[The resonance Raman spectrum of cyclobutene](#)

J. Chem. Phys. **103**, 5911 (1995); 10.1063/1.470471

[Stimulated Raman Spectrum of Cyclohexane](#)

J. Appl. Phys. **37**, 4996 (1966); 10.1063/1.1708180

[Phonon Spectrum of Graphite](#)

J. Chem. Phys. **42**, 357 (1965); 10.1063/1.1695699

**AIP** | APL Photonics

*APL Photonics* is pleased to announce  
**Benjamin Eggleton** as its Editor-in-Chief



## Raman Spectrum of Graphite

F. TUINSTR\* AND J. L. KOENIG

*Division of Macromolecular Science, Case Western Reserve University, Cleveland, Ohio 44106*

(Received 13 November 1969)

Raman spectra are reported from single crystals of graphite and other graphite materials. Single crystals of graphite show one single line at  $1575\text{ cm}^{-1}$ . For the other materials like stress-annealed pyrolytic graphite, commercial graphites, activated charcoal, lampblack, and vitreous carbon another line is detected at  $1355\text{ cm}^{-1}$ . The Raman intensity of this band is inversely proportional to the crystallite size and is caused by a breakdown of the  $k$ -selection rule. The intensity of this band allows an estimate of the crystallite size in the surface layer of any carbon sample. Two in-plane force constants are calculated from the frequencies.

### INTRODUCTION

Before the advent of the laser as a Raman source, Raman spectroscopy of completely black materials like carbon black and graphite was not possible. With the use of powerful lasers, a spectroscopic study of these black materials seemed appropriate. We have succeeded in obtaining the spectra of single crystals of graphite as well as of microcrystalline graphite samples.

A renewed interest in the structural properties of graphitized materials has been generated by their potential use as a reinforcing material in the form of fibers and whiskers. In these materials the structure of the fiber surface plays a critical role in the application. As will be shown in the present paper Raman spectroscopy is a promising tool for characterization of graphite surface.

The lattice dynamics of graphite has been treated theoretically several times in the past.<sup>1,2,3</sup> Lack of accurate data, mainly due to lack of big single crystals of graphite,<sup>4</sup> always left some ambiguity in the force constants even for a simple potential field.<sup>1,3</sup> By using Raman scattering one can get accurate data without the use of large crystals. The results of a more precise determination of some of the force constants will be discussed.

### EXPERIMENTAL

The  $4880\text{-}\text{\AA}$  line ( $\sim 300\text{ mW}$ ) of an Ar-ion laser was used to induce the Raman spectrum. The  $5145\text{-}\text{\AA}$  line was used on occasion.

The scattered light was observed under  $90^\circ$  with the incident beam. To resolve the Raman from the Rayleigh scattering, a double monochromator (Spex 1400) was used. At the exit slit, photon counting converted the signal into the input voltage for the recorder.

The single crystals of graphite were mounted on a goniometer head to observe the Raman scattering at different orientations of the crystal with respect to the incident beam. The microcrystalline samples were pressed into pellets. The pellets were mounted so the incident beam made an angle of  $30^\circ$  with the flat front surface.

The laser beam was focused on the surface of the samples. With the aid of a microscope, which was mounted on top of the sample holder, the illuminated area of the sample could be examined *in situ*. The mi-

croscope also allowed a selection of the illuminated area and a control of its size. The illuminated area could be reduced to  $10\text{ }\mu\text{m}$  in diameter. The high light intensity makes observation of the Raman spectrum of graphite possible.

Because of the absorption of the light in the graphite, the observed spectra are induced in a thin surface layer. The incident and scattered intensity are reduced to  $1/e$ , where  $e$  is the base of the natural system of logarithms, after passing a layer of the order of  $0.05\text{ }\mu\text{m}$  of graphite.

The spectra were run while the sample was in a helium atmosphere to rid the spectra of gases in the air.

### RESULTS

The Raman spectrum of single crystals of graphite is shown in Fig. 1. The single crystals need only be larger than the area illuminated by the laser beam, i.e.,  $20\text{ }\mu\text{m}$ . Different samples gave exactly the same spectrum. Natural graphite (Madagascar flakes and Ticonderoga crystals) was used because of its large crystal size. The only Raman line observed occurs at  $1575\text{ cm}^{-1}$ . Different orientation of the sample with respect to the incident beam did not change the spectrum. Polarization measurements were attempted but no polarization was detected. Whether the line at  $1575\text{ cm}^{-1}$  is polarized or depolarized cannot be determined at this time, perhaps due to the high internal scattering in the samples.

In the Raman spectrum of all other graphitic materials like activated charcoal, carbon black, and vitreous carbon a second line appears as Fig. 2 illustrates. The additional line is observed near  $1355\text{ cm}^{-1}$ . The relative intensities of the two lines depend on the type of graphitic material. The intensity of the  $1355\text{ cm}^{-1}$  line increases as one goes from stress annealed pyrolytic graphite through commercial graphite to carbon black. This increase corresponds (i) with an increase in the amount of "unorganized" carbon in the samples and (ii) with a decrease in the graphite crystal size.

### DISCUSSION

#### Single Crystals of Graphite

Hexagonal graphite has a crystal structure built up of flat layers in which the trivalent carbon atoms occupy

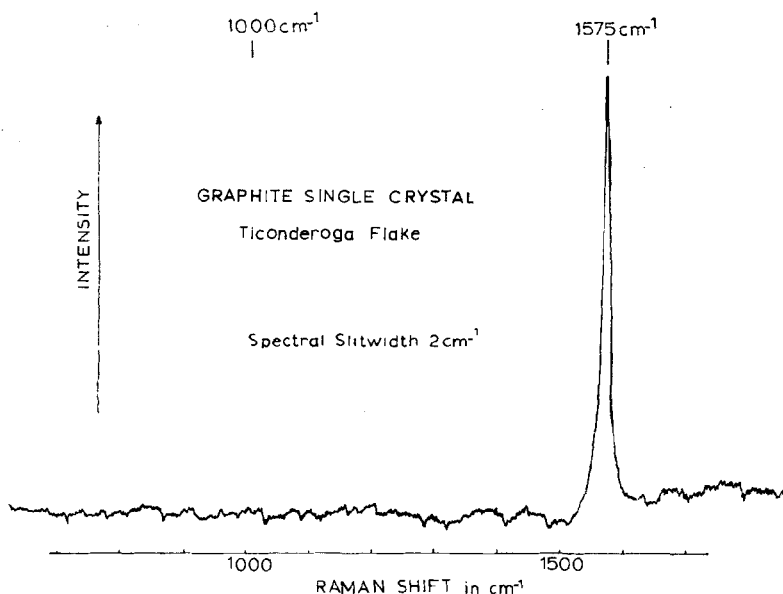


FIG. 1. Raman spectrum of a single crystal of graphite.

the lattice sites of a two-dimensional honeycomb network. The layers are stacked in a hexagonal crystal structure corresponding to the space group  $P6_3/mmc (= D_{6h}^4)$ . The unit cell contains four atoms: two from each of the contributing layers. In single crystals of graphite, the shortest interatomic distance is 1.42 Å in the planes, while the distance between the consecutive planes is 3.354 Å. In other types of graphite, the covalent bond distance of 1.42 Å is always preserved, but the interlayer distance can have values ranging from 3.354 Å up to 3.7 Å. With this loss of packing density, a loss in the three-dimensional crystallinity is observed. The layers stay perfectly parallel but their mutual orientation in the direction of the planes is random (turbostatic).

The Raman line at 1575  $\text{cm}^{-1}$  is present in all of the graphite samples studied. A slight frequency shift ( $\sim 15 \text{ cm}^{-1}$ ) toward higher wavenumber was found in some samples with extremely small crystal sizes. This band does not depend on the mutual arrangement of the graphite planes since it appears at the same frequency in those graphite samples with only two-dimensional crystallinity.

The number of frequencies expected in the Raman spectrum of single crystals of graphite can easily be enumerated. There are four atoms in the unit cell so the phonon dispersion relation will reveal nine optical branches. Raman (or infrared) activity for a crystal can only be observed in the limit where the wave vector  $\mathbf{k}=0$ . The unit cell has a symmetry consistent with the space group  $D_{6h}^4$ . The point group homomorphic with this space group is  $D_{6h}$ . From the properties of this point group and the requirement that all unit cells must vibrate with the same phase ( $\mathbf{k}=0$  or corresponding to the totally symmetric mode of the translation lattice), the symmetry properties of the normal modes can be

calculated. The results are

$$2B_{2g} + 2E_{2g} + A_{2u} + E_{1u}.$$

Only the  $2E_{2g}$  modes are expected to be Raman active as fundamentals. The symmetry of the  $E_{2g}$  modes restricts the motion of the atoms to the plane of the carbon atoms. The two different  $E_{2g}$  modes in this three-dimensional analysis occur because adjacent planes can vibrate in phase or with opposite phase. The difference in energy between the two  $E_{2g}$  modes will be very small due to the relatively weak interlayer forces. In single crystals of graphite, the two  $E_{2g}$  modes will probably not show a measurable frequency separation and will appear as one single band. The Raman band observed in single crystals of graphite can be assigned to these  $E_{2g}$  modes.

For graphitic materials other than single crystals, an analysis using only one layer of atoms seems more appropriate. For a unit cell containing only 2 atoms, the analysis gives for the resulting modes:

$$B_{2g} \text{ and } E_{2g}.$$

Only the  $E_{2g}$  is Raman active, so only one band is expected in the two-dimensional analysis.

Since only one band is expected in the Raman spectrum, it is desirable to calculate the frequency of the  $E_{2g}$  mode to assure ourselves that the observed mode falls in the appropriate frequency range. Due to the weak interlayer forces, the vibrational analysis can be restricted to a two-dimensional analysis of the in-plane motions of the hexagonal "honeycomb" network. This method now applies to all graphitic materials including single crystals. A modification<sup>5</sup> of the Wilson GF method is used which leads to a secular equation of the type

$$|A - \lambda E| = 0,$$

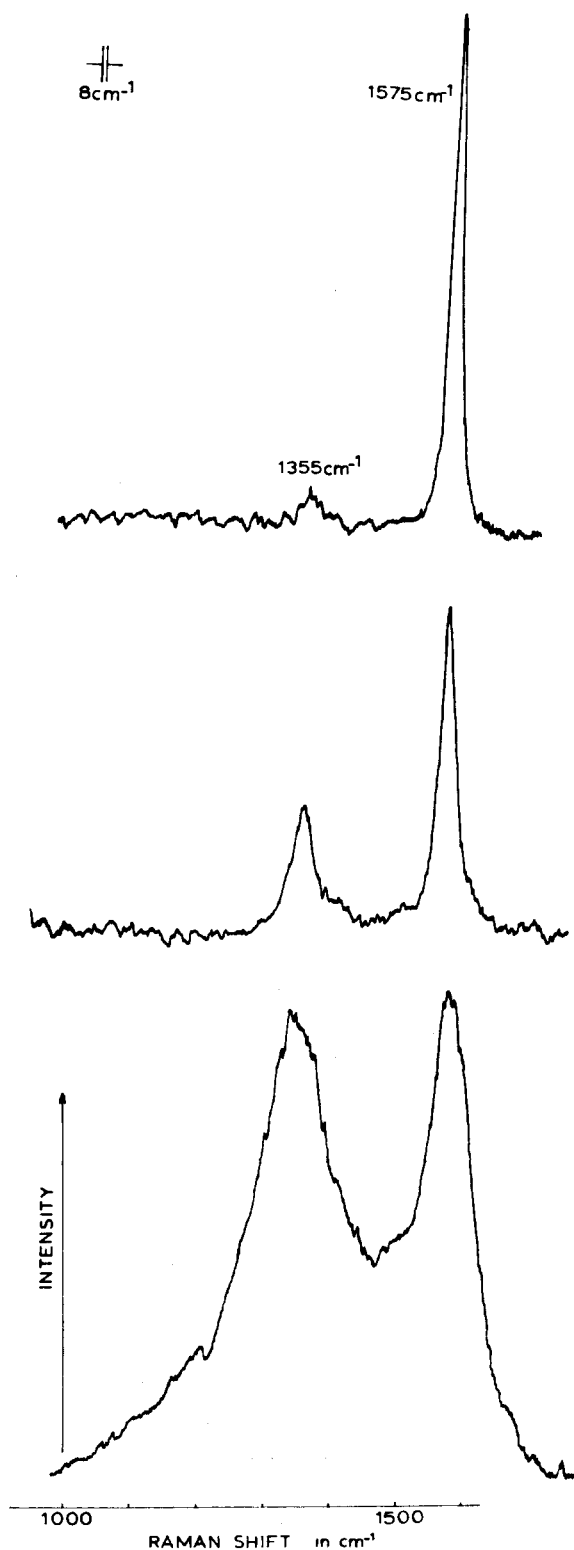


FIG. 2. Comparison of the Raman spectra of (A) stress-annealed pyrolytic graphite, (B) a commercial graphite, and (C) activated charcoal.

where

$$A = UB'FBU',$$

with  $F$  the potential energy matrix in internal coordinates and  $B$  the mass-adjusted transformation matrix from Cartesian to internal coordinates and  $U$  changes the Cartesian coordinates into external symmetry coordinates.

The resulting secular equation reduces to

$$(1/M_e)(3K + 18H) = \lambda,$$

a result that also can be obtained by application of the formulas of Yoshimori and Kitano.<sup>1</sup> Using approximate force constants recently reported,<sup>3</sup> the approximate frequency of the  $E_{2g}$  mode is  $1688 \text{ cm}^{-1}$ . This calculated

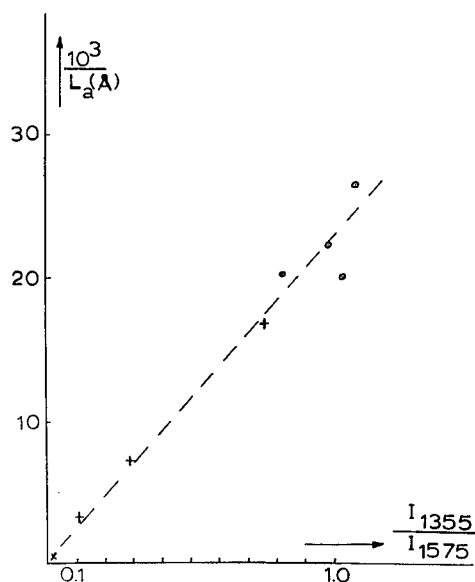


FIG. 3. Calibration of Raman intensities versus x-ray data of  $L_a$ . O, data and samples furnished by Dr. S. L. Strong (Union Carbide). +, samples prepared following directions in [G. M. Arnold, carbon 5, 33 (1967)]. X, stress annealed pyrolytic graphite.

frequency is in reasonable agreement (considering the approximate force constants) with the single line observed at  $1575 \text{ cm}^{-1}$ . This calculation gives us additional evidence for assignment of the band at  $1575 \text{ cm}^{-1}$  to the degenerate  $E_{2g}$  mode.

### Graphitic Materials

The Raman spectra of the other graphitic materials show a line at  $1355 \text{ cm}^{-1}$  in addition to the omnipresent line near  $1575 \text{ cm}^{-1}$ .

Polarization effects were observed only for stress annealed pyrolytic graphite. In this case the effect was detected only if the incident laser beam was aimed at a clean surface which is cut parallel to the  $c$  axis. Both lines appeared to be strong only if the incident beam was polarized parallel to the graphite planes. The scattered light appeared to be polarized in the same way.

These observations are in agreement with the assignment of the  $1575\text{ cm}^{-1}$  to the  $E_{2g}$  mode. It should be noted that from the geometry of the sample mounting, the angle between the incident and scattered light is about  $40^\circ$ , due to the refractive index of the sample.

There is a marked change in the relative scattering intensities of the two lines for samples of different type and origin. Since the  $1355\text{-cm}^{-1}$  line cannot be explained from the analysis previously presented, another origin for this line must be sought.

Impurities as a source of this  $1355\text{-cm}^{-1}$  line can be excluded on the basis that the  $1355\text{-cm}^{-1}$  line does not correspond to any of the frequencies found in the infrared measurements on carbons<sup>6</sup> and the impurity concentration is very low in some of these samples. Additionally, we have heated a sample on the sample stage of the spectrometer up to some  $1200^\circ\text{C}$  while it was immersed in a He atmosphere. The spectrum was run right after the heating cycle. The spectrum did not show any change.

When a comparison is made with the Raman spectrum of diamond, a simple explanation for the  $1355\text{ cm}^{-1}$  line suggests itself. Only a single band is observed in the Raman spectrum of diamond at  $1332\text{ cm}^{-1}$ . The  $1355\text{ cm}^{-1}$ -line might possibly be due to a diamondlike atomic arrangement in the graphite samples. Those atoms not located in the graphite layers are probably partially tetrahedrally bonded. However, closer examination rules out this possibility, for the following reasons:

(i) The intensity changes of the  $1355\text{-cm}^{-1}$  line are not linear with the inverse of the unorganized carbon content.

(ii) The  $1355\text{ cm}^{-1}$  line has a narrow bandwidth, whereas the "nonorganized carbon," which is highly disordered,<sup>7</sup> should give a broad line.

(iii) We would expect a frequency shift downward from  $1332\text{ cm}^{-1}$  instead of the observed shift, both from the distortion of the bonds and from a heating effect due to the laser radiation.<sup>8</sup>

(iv) Diamond powder graphitized in the laser beam. Diamondlike structures are not expected to survive exposure to the focused laser beam.

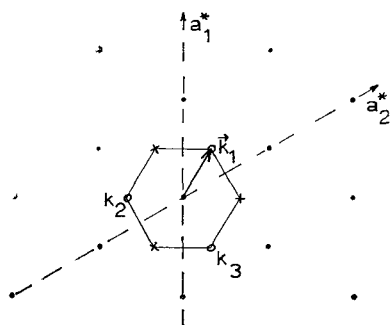


FIG. 4. First Brillouin zone of the two-dimensional graphite lattice.  $k_1 = k_2 = k_3$ .

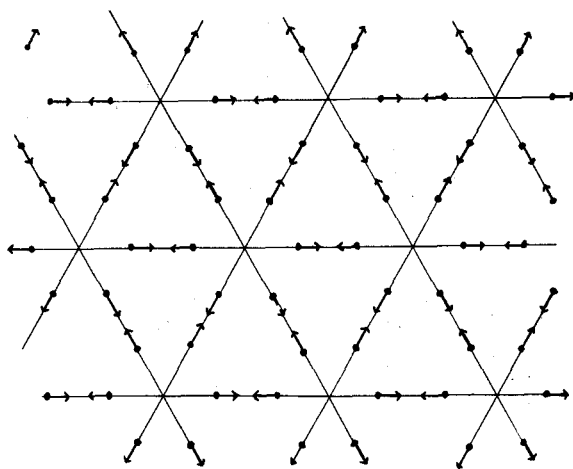


FIG. 5.  $A_{1g}$  mode which is Raman active in "finite" crystallites only.

(v) Unorganized carbon would not account for the polarization effects observed for the  $1355\text{-cm}^{-1}$  line.

The other possible explanation of the occurrence of the  $1355\text{-cm}^{-1}$  line already suggested is a particle size effect. In Fig. 3 the Raman intensity is plotted versus  $1/L_a$ , where the crystallite size  $L_a$  is obtained from x-ray data. The linear relationship shows that the Raman intensity is proportional to the percentage of "boundary" in the sample. Another way to observe the effect is by grinding stress-annealed pyrolytic graphite; in this way the intensity of the  $1355\text{-cm}^{-1}$  band can be increased to a certain limit. The plot in Fig. 3 can now be used to determine  $L_a$  in the thin surface layer of a graphite sample.

We attribute now the  $1355\text{-cm}^{-1}$  line to a change in the selection rules for Raman activity of certain phonons which were inactive in the infinite lattice. For polymers, end effects produce spectral differences of this type.<sup>9</sup>

Looking at these small crystallites as big molecules with different sizes and shapes, the only new Raman active modes are of the  $A_{1g}$  type.

In Fig. 4 the first Brillouin zone of the two-dimensional graphite lattice is shown in reciprocal space. All of the points inside the zone or on the boundary represent possible phonons. Due to the irregular boundaries we can reject standing waves resulting from reflection at the boundaries, so we are left with phonons corresponding to the point  $\mathbf{k}=0$  and the boundaries of the first zone which represent internal standing waves. The point  $\mathbf{k}=0$  has the full symmetry of the lattice,  $D_{6h}$ , and gives rise to the  $E_{2g}$  Raman mode. The only other point that has symmetry high enough to give rise to an  $A_{1g}$  mode is the point  $\mathbf{k}_1$ . This point is equivalent to points  $\mathbf{k}_2$  and  $\mathbf{k}_3$ . These corresponding points in reciprocal space have symmetry  $D_{3h}$ .

From the secular equation, the eigenvalues and eigenvectors can be calculated. These eigenvectors show that there is an  $A_{1g}$ -type of mode at the  $\mathbf{k}_1$  point. This

mode is depicted in Fig. 5. In an infinite crystal, this mode will be Raman inactive because the changes in polarizability cancel over the infinite crystal. For small crystallites, this is not true, and Raman activity can be observed. We attribute the  $1355\text{-cm}^{-1}$  line of graphite to this  $A_{1g}$  mode of the small crystallites, or boundaries of larger crystallites. The observed polarization effects in stress-annealed pyrolytic graphite are in accordance with this assignment.

The eigenvalues obtained for the point  $k_1$  correspond exactly with the results of the treatment of Yoshimori and Kitano<sup>1</sup> if the appropriate parameters for  $k_1$  are used. This  $A_{1g}$  mode corresponds to a longitudinal acoustic mode for the infinite lattice. The eigenvalue is  $\lambda = 3K/M_c$ , where  $K$  is the bond stretching force constant and  $M_c$  is the mass of the carbon atom. From Fig. 5, it also can be seen that in this mode, no change in the bond angles occurs so the force constant involving deformation of the angle is not involved.

Since two different Raman lines due to in-plane motions of the carbons are observed, it is possible to calculate two force constants. The bond stretching force constant,  $K$ , can be determined directly from the  $1355\text{-cm}^{-1}$  line and has a value of  $4.32 \times 10^5$  dyn/cm. Inserting this value in the expression for the eigenvalue of the  $1575\text{-cm}^{-1}$  line, we can calculate the force constant for the deformation of the angle,  $H$ , which has a calculated value of  $0.25 \times 10^5$  dyn/cm.

In the literature, different values for the force constants have been reported. A set of values can be obtained from the observed elastic force constants  $c_{11}$  and  $c_{12}$ <sup>10</sup>; the corresponding values for  $K$  and  $H$  are  $7.1 \times 10^5$  and  $0.67 \times 10^5$  dyn/cm, respectively. Yoshimori and Kitano used  $K = 6.71$  and  $H = 0.48 \times 10^5$  dyn/cm (see also Ref. 11), while Young and Koppel found that values of  $K = 4.36$  and  $H = 0.38 \times 10^5$  dyn/cm fitted the specific heat data. The present value of  $H$  is lower than the one reported by Young and Koppel. Although an excellent fit to the specific heat was found by the latter authors, it is our opinion that the simple force field introduced by Yoshimori and Kitano is not adequate to describe the phonon dispersion curves in detail.

## CONCLUSIONS

The Raman spectra of single crystals of graphite shows only one mode at  $1575\text{ cm}^{-1}$  which is assigned to

the  $E_{2g}$  species of the infinite crystal. Polycrystalline graphite exhibits another band at  $1355\text{ cm}^{-1}$ . The intensity of the latter is inversely proportional to the effective crystallite size  $L_a$  in the direction of the graphite plane. The  $1355\text{-cm}^{-1}$  band is attributed to a particle size effect. Due to the finite crystal size, an  $A_{1g}$  mode of the lattice becomes Raman active. The intensity of this band allows the measurement of  $L_a$  in a thin surface layer of any carbon sample. Theoretical analysis of these bands allows a determination of two in-plane force constants. The C-C bond stretching force constant has a calculated value of  $4.32 \times 10^5$  dyn/cm, which is in excellent agreement with results obtained by other workers from specific heat measurements.<sup>3</sup> The second force constant corresponds to angle deformation and has a value of  $0.25 \times 10^5$  dyn/cm which is lower than the previously reported values. It appears from a comparison with other reported force constants that the Yoshimori and Kitano force field is not sufficient to give precise phonon dispersion curves.

## ACKNOWLEDGMENT

The authors gratefully acknowledge the support of Advanced Research Projects Agency, Department of Defense, through a contract with the Air Force Materials Laboratory, Wright-Patterson Air Force Base, Ohio. The samples for this research were kindly supplied by Union Carbide Company at the Parma Technical Center.

\* On leave from Physics Department, Technical University, Delft, Netherlands.

<sup>1</sup> A. Yoshimori and Y. Kitano, J. Phys. Soc. Japan 2, 352 (1956).

<sup>2</sup> C. Champier, J. M. Genin, and C. Janot, Compt. Rend. 257, 1843 (1963).

<sup>3</sup> J. A. Young and J. U. Koppel, J. Chem. Phys. 42, 357 (1965).

<sup>4</sup> G. Dolling and B. N. Brockhouse, Phys. Rev. 128, 1120 (1962).

<sup>5</sup> See for instance: T. Shimanouchi, M. Tsoboi, and T. Miyazawa, J. Chem. Phys. 35, 1597 (1961).

<sup>6</sup> J. Mattson and H. B. Mark, Jr., 43rd National Colloid Symposium, Cleveland, Ohio, June 23-25, 1969, Paper 58.

<sup>7</sup> R. E. Franklin, Proc. Roy. Soc. (London) A209, 196 (1954).

<sup>8</sup> R. S. Krishnan, Proc. Indian Acad. Sci. 24, 45 (1946).

<sup>9</sup> R. F. Schaufele and T. Shimanouchi, J. Chem. Phys. 47, 3605 (1967).

<sup>10</sup> G. B. Spence and E. J. Seldin as quoted by W. N. Reynolds, *Physical Properties of Graphite* (Elsevier, London, 1968), p. 35.

<sup>11</sup> From neutron scattering data D. H. Saunderson, as quoted by Reynolds (Ref. 10, p. 72), concludes that this  $K$  is about 10%-20% too high.